Single Axis Geometry by Fitting Conics

No Author Given

No Institute Given

Abstract. In this paper, we describe a new approach for recovering 3D geometry from an uncalibrated image sequence of a single axis (turntable) motion. Unlike previous methods, the computation of multiple views encoded by the fundamental matrix or trifocal tensor is not required. Instead, the new approach is based on fitting a conic locus to corresponding image points over multiple views. It is then shown that the geometry of single axis motion can be recovered given at least two such conics. In the case of two conics the reconstruction may have a two fold ambiguity, but this ambiguity is removed if three or more conics are used.

The approach enables the geometry of the single axis motion (the 3D rotation axis and Euclidean geometry in planes perpendicular to this axis) to be estimated using the minimal number or parameters. It is demonstrated that a Maximum Likelihood Estimation results in measurements that are as good as or superior to those obtained by previous methods, and with a far simpler algorithm. Examples are given on various real sequences, which show the accuracy and robustness of the new algorithm.

1 Introduction

Acquiring 3D models from a single axis motion sequences, particularly turntables, has been widely used by computer vision and graphics researchers. The key component of the 3D reconstruction based on a single axis motion sequences is the recovery of rotation angles. Traditionally, rotation angles are obtained by careful calibration [?],[?],[?],[?]. Fitzgibbon et al. [?] extended this approach to recover unknown rotation angles based on a projective geometry approach. In their method, corresponding points are carefully tracked from each pair of images for the fundamental matrices and each triplet of images for the trifocal tensors, which makes the method complicated. Mendonça et al. [?] recover the rotation angles from profiles of surfaces. The search of corresponding point is transformed into search for epipolar tangencies, which involves a nonlinear optimization. All the above papers have discussion on some invariants in this special single axis motion. However the ideal points $\mathbf{i}$ and $\mathbf{j}$, which play a very important role in rotation angle recovery is omitted.

Recently we have proposed a new approach which does not need to compute trifocal tensor [?],[?],[?]. Instead, the corresponding points in different images are fitted to a conic. It is then shown that rotation angle can be directly computed from only one conic and one fundamental matrix. The remaining geometric quantities can be obtained using more conics [?]. In this paper, we further show that even the one fundamental matrix is unnecessary. All single axis geometry can be computed from at least two conics by directly calculating the image of the circular points. Then all invariant quantities of the single axis motion can be computed. The advantage of the new method over the existing ones is straightforward. First, it is intrinsically a multiple view approach as all geometric information from the whole sequence is nicely summarized in the conics! Unlike the computation of fundamental matrices and trifocal tensors which use only a subsequence of 2 and 3 views respectively. Second, we are determining a series of 5 conic parameters from N views instead of a series of 7 fundamental matrix parameters from 2 views plus a series of 18 tensor parameters from 3 views. It is obvious that the algorithm is much more simple and robust.

The paper is organized as follows. A review of the geometry of the single axis motion is given in Section **??**. Section **??** describes the invariants under the single axis motion case and the rotation angles recover based on these invariants. A Maximum Likelihood Estimation method for these invariants and conics fitting is given in Section **??**. Section **??** demonstrates two experiments. One is on the reconstruction of the Hannover dinosaur from a turntable image sequence. The other is on a reconstruction of a girl who is seating in a rotating chair. The later is a short video sequence and we want to show that 3D photography can be easily done. Finally, a short conclusion is given in Section **??**.

2 Review of the Geometry of single axis motion

Throughout the paper, scalars are denoted in any plain letters or lower case Greek. Assuming a pin-hole camera model, the object space may be considered as embedded in $\mathcal{P}^3$ and the image space embedded in $\mathcal{P}^2$. Vectors in $\mathcal{P}^2$ are denoted in lower case boldface and vectors in $\mathcal{P}^3$ and matrices in upper case boldface. The camera performs the projection from $\mathcal{P}^3$ to $\mathcal{P}^2$, and can be represented by a 3×4 matrix $\mathbf{P}_{3\times 4}$ of rank 3 whose kernel is the projection center. The relationship between a point $\mathbf{X}$ in $\mathcal{P}^3$ and a point $\mathbf{u}$ in $\mathcal{P}^2$ can be written as

$$\lambda \mathbf{u} = \mathbf{P}_{3\times 4}\mathbf{X}, \tag{1}$$

where $\mathbf{u}$ and $\mathbf{X}$ are in homogeneous coordinates and λ is a non-zero scalar.

A typical set up for single axis motion consists of a stationary CCD camera in front of a turntable on which the object to be reconstructed is placed [?], [?]. The internal parameters of the camera are assumed fixed.

For a single axis motion, without loss of generality, the rotation axis of the turntable is chosen to be the z-axis the world coordinate. Then each point on the object is moving in its plane that is pendicular to the z-axis. Indeed, there is a pencil of horizontal planes. The invariants related to the geometry of single axis motion have been established in [?]. These invariants on the image plane are:

1. The line $\mathbf{l}_s$ which is the image of the rotation axis.

2. The line $\mathbf{l}_\infty$ which is the intersection line for all horizontal planes. Actually, it is the vanishing line of all the horizontal planes.
3. The point $\mathbf{x}_s$ which is the image of the cross point of the lines $\mathbf{l}_s$ and $\mathbf{l}_\infty$.
4. The point $\mathbf{v}$ which is the vanishing point of the rotation axis.

These fixed image entities are illustrated schematically in Figure **??**.

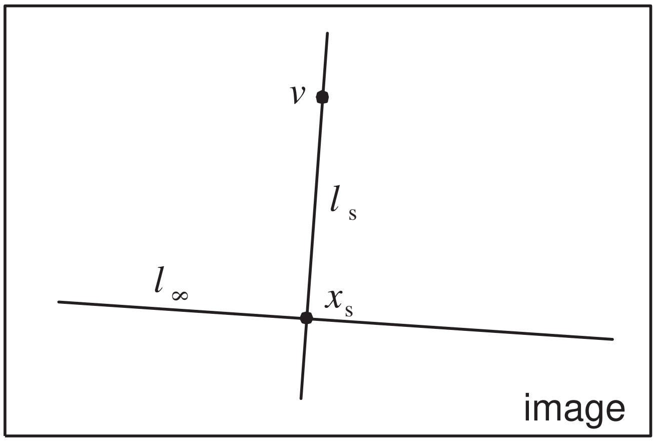

Fig. 1. Fixed image entities

3 Single Axis Geometry and Conic Loci

Our first remark is that the trajectory of the corresponding points in different images of any given space point, displayed in any particular image plane is a conic by the very definition of single axis motion (Figure **??**). This extremely trivial observation that the previous methods fail to exploit is the starting point of our new methods of determining single axis geometry from conic loci. Traditional methods that require the estimation of pair-wise fundamental matrices and triplet trifocal tensors from the corresponding points in different views. We have previously proposed a method in which needs only to estimate one pair-wise fundamental matrix, then to fit a conic to the corresponding points in at least 5 images [**?**]. Actually, it turns out that we can compute the geometry by just fitting of conics to the tracked points over at least five images. A minimum of 2 conics is necessary to recover the whole geometry of single axis motion.

3.1 Computing the image of the circular points from conics

The first essential observation is that all conic locus of image points of an object from a single axis motion are going through the image of the circular points.

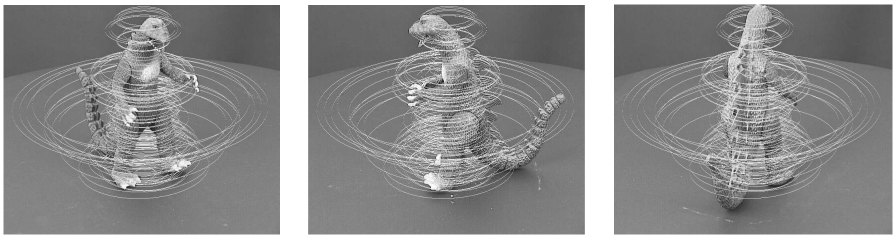

Fig. 2. Dinosaur sequence and Conics

This can be easily proved by the fact that the trajectory of a given object point in space from a single axis motion is always a circle and different points therefore give circles of different radius on different planes which are all parallel and perpendicular to the single rotation axis. All circles go through their respective circular points of the plane they are lying on by the very definition of the circular points [?]. As all these supporting planes are parallel, i.e. they are sharing the common line at infinity on which the circular points lie. We may thus conclude that all circles of different radius on different parallel planes from the single axis motion are sharing the common pair of circular points $\mathbf{i}$ and $\mathbf{j}$. Because that this is a projective property, so it remains true for the projection onto any image plane. In any particular image plane, this means that all conic loci of corresponding points are intersecting in the pair of common circular points $\mathbf{i}$ and $\mathbf{j}$. Thus, by just computing intersection points of at least two conic loci, we obtain the image of circular points, and also the vanishing line of the parallel planes.

Consider the intersection of a pair of conics. it always has 4 intersection points including complex and infinite points according Bezout theorem. In terms of real intersection points, they may have 0, 1, 2, 3, or 4 according to the configurations.

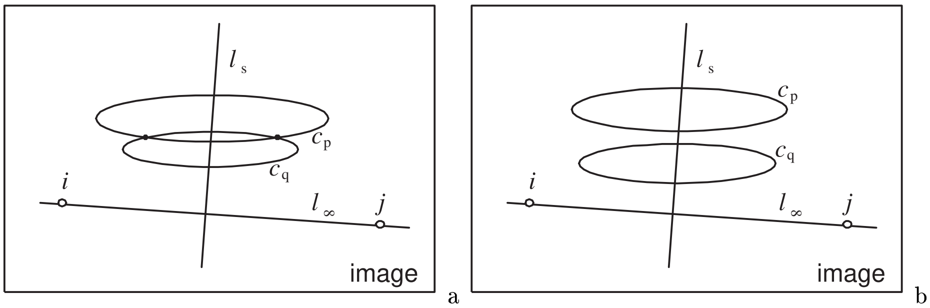

Fig. 3. The intersections of two conics

– For the case of 1 or 2 real intersection points, it is straightforward that the only pair of complex conjugate points is the image of the circular points.
– It is generally impossible to have 3 or 4 real intersection points if the conics are real perspective image of the circles from the single axis motion by its definition.
– The most difficult case is that there is no real intersection points. This is in fact very common if we just look at the illustrative conic loci in Figure **??**. In this case, we obtain two pairs of complex conjugate points. There is a reconstruction ambiguity coming from the ambiguity of the two pairs of complex conjugate points. Of course, this ambiguity could be immediately removed as soon as we have more than 2 conics.

3.2 The complete computation method

After having described the key components of computing the image of the circular points from at least two conics, we can summarize the complete method of computing rotational angles and the underlying single axis geometry.

1. Fit two conics $\mathbf{C}_p$ and $\mathbf{C}_q$ to all tracked points over the sequence for two given points respectively. At this stage, two points tracked over at least 5 images are needed.
2. Compute the intersection points of the two conics $\mathbf{C}_p$ and $\mathbf{C}_q$. We may have either one pair of complex conjugates or two pairs of complex conjugates. If there is a unique pair of complex conjugates, the image of circular points $\mathbf{i}$ and $\mathbf{j}$ are exactly this pair of complex conjugates. However if there are two possible pairs of complex conjugate points, we obtain two possible solutions. This double solution ambiguity can be removed by using any additional conic.
3. Compute the vanishing line
$$\mathbf{l}_\infty = \mathbf{i} \times \mathbf{j}.$$
4. Obtain the projection of the two circle centers as the pole of the line $\mathbf{l}_\infty$
$$\mathbf{o}_p = \mathbf{C}_p^{-1}\mathbf{l}_\infty,$$
$$\mathbf{o}_q = \mathbf{C}_q^{-1}\mathbf{l}_\infty.$$
5. It is clear that the rotation axis is
$$\mathbf{l}_s = \mathbf{o}_p \times \mathbf{o}_q.$$
6. Compute the angular motion between two views from the tracked points. i.e. points $\mathbf{a}$ and $\mathbf{b}$ on two views are tracked points on conic $\mathbf{C}_p$, the rotation angle of the two views can be calculated by using Laguerre's formula [**?**]
$$\theta_{ab} = \frac{1}{2i}\log(\{\mathbf{l}_{o_p a}, \mathbf{l}_{o_p b}; \mathbf{l}_{o_p i}, \mathbf{l}_{o_p j}\}).$$

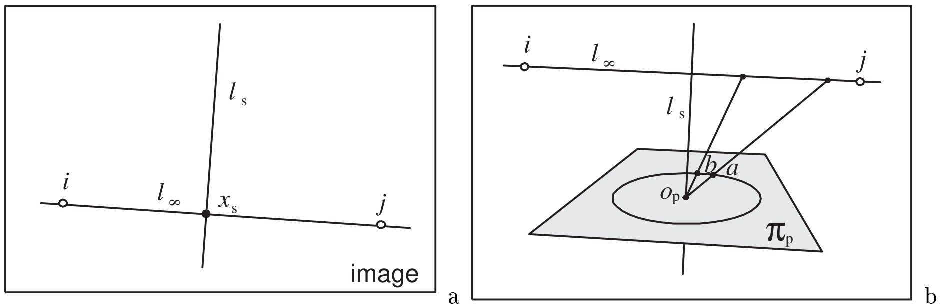

Fig. 4. (a)Fixed image entities deduced from conics. (b)The the rotation angle with respected to the image entities.

The fixed image entities for the single axis motion deduced from two conics are shown in Figure **??**.a and the the rotation angle with respected to the image entities is shown in Figure **??**.b.

Compare with the Figure **??**, the vanishing point $\mathbf{v}$ of the rotation axis cannot be obtained from the conics. That mean although metric structures in all planes perpendicular rotation axis can be accurately determined, the reconstruction along the rotation axis is a 1D projective one. This same result is also shown by Fitzgibbon et al. [**?**] and other researchers [**?**], [**?**], [**?**] which have two parameters not determined. The ambiguity can be removed by specifying camera aspect ratio and parallel scene lines.

3.3 Recover lost angles

In practice, sometimes what we tracked several points are all missed in some views. Then, the rotation angles with respect to the views cannot be recovered. In this part, we show how to find the lost corresponding points and how to recover these lost angles.

Figure **??** illustrates this configuration to help the following development. The conic $\mathbf{C}$ on the plane π_1 has been obtained from at least five images. The point $\mathbf{a}$ is visible in the views m_1 and m_2 as $\mathbf{a}_1$ and $\mathbf{a}_2$, but missing in the view m_3. The point $\mathbf{a}_3$ is not available. However a point $\mathbf{b}$ is available in three views m_1, m_2, and m_3 as $\mathbf{b}_1$, $\mathbf{b}_2$ and $\mathbf{b}_3$. Let us assume its unknown conic trajectory be the conic $\mathbf{C}_i$ on the plane π_i. The two planes π_1 and π_i are parallel in the world coordinates, they share the same vanishing line $\mathbf{l}_\infty$ and the two circular points $\mathbf{i}$ and $\mathbf{j}$. Since the rotation angle between the view m_1 and m_2 is known from the conic $\mathbf{C}$. We may rewrite the Laguerre's formula for the point $\mathbf{b}$ on the plane π_i:

$$\theta_{12} = \frac{1}{2i} \log(\{\mathbf{l}_{o_1 b_1}, \mathbf{l}_{o_1 b_2}; \mathbf{l}_{o_1 i}, \mathbf{l}_{o_1 j}\}),$$

where the point $\mathbf{o}_1$ is the only unknown vector of the image of the circle center. Since $\mathbf{o}_1$ lies on $\mathbf{l}_s$, the one unknown component of this point can be calculated from the known cross ratio $\{\mathbf{l}_{o_1b_1}, \mathbf{l}_{o_1b_2}; \mathbf{l}_{o_1i}, \mathbf{l}_{o_1j}\}$.

From the reconstructed point $\mathbf{o}_1$, the rotation angle θ_{23} between the view m_2 and m_3 can be obtained.

$$\theta_{23} = \frac{1}{2i}\log(\{\mathbf{l}_{o_1b_2}, \mathbf{l}_{o_1b_3}; \mathbf{l}_{o_1i}, \mathbf{l}_{o_1j}\}),$$

After the determination of the angle θ_{23}, again apply the Laguerre's formula to calculate the line $\mathbf{l}_{oa_3}$. By intersecting the line $\mathbf{l}_{oa_3}$ with the conic $\mathbf{C}$, the missing point $\mathbf{a}_3$ can be recovered.

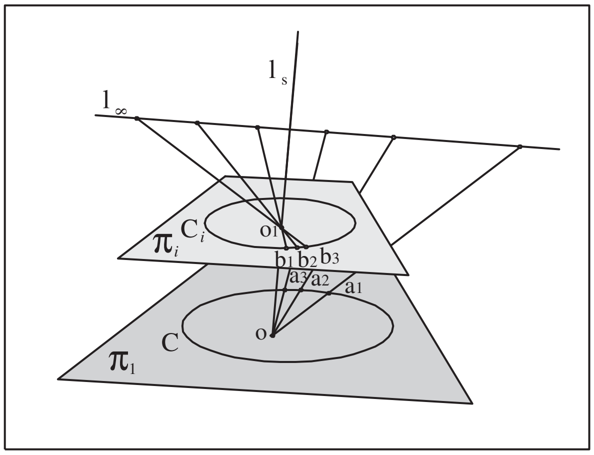

Fig. 5. Finding missing points and recover lost angles.

4 Invariants estimation and conics fitting based on Maximum Likelihood Estimation

It is shown that the geometry of single axis motion can be recovered given at least two conics. In the case of two conics the reconstruction may have a two fold ambiguity, three or more conics can be used. In this section, a Maximum Likelihood Estimation(MLE) method is given for the invariants estimation and conics fitting.

4.1 Dof for the MLE

As mentioned early, each point on the object is moving in its plane that pendicular to the z-axis and there are a pencil of horizontal planes. For each such plane, there is a plane homography $\mathbf{H}$ which maps the conic in the image plane to the circle lies in the horizontal plane,

$$\mathbf{C}_{irle} = \mathbf{H}^{-T}\mathbf{C}_{onic}\mathbf{H}^{-1}. \tag{2}$$

And we assume the center of the circle lies in the original point of the plane and the radius is one.

The homography can be decomposed into a concatenation of five matrices $\mathbf{R}$, $\mathbf{S}$, $\mathbf{T}$, $\mathbf{A}$ and $\mathbf{P}_u$, representing rotation, isotropic scaling, translation, affine and 'pure projective' transformation respectively ([?],[?],[?]):

$$\mathbf{H} = \mathbf{RSTAP}_u. \tag{3}$$

where

$$\mathbf{P}_u = \begin{bmatrix} 1 & 0 & 0 \\ 0 & 1 & 0 \\ l_1 & l_2 & l_3 \end{bmatrix},$$

can be determined by the vanishing line $\mathbf{l}_\infty = (l_1, l_2, l_3)$.

$$\mathbf{A} = \begin{bmatrix} \frac{1}{\beta} & -\frac{\alpha}{\beta} & 0 \\ 0 & 1 & 0 \\ 0 & 0 & 1 \end{bmatrix},$$

$(\alpha \mp i\beta, 1, 0)^T$ is the circular points on the affine plane which can be obtained by $\mathbf{P}_u$ multiply by circular points $\mathbf{i}$ and $\mathbf{j}$. It is clear that the degree of freedom of the circular points is four. Two determine the 'pure projective' matrix and two determine the affine matrix. As shown in Figure 4, the other fixed image entity is the rotation axis $\mathbf{l}_s$, which has two degree of freedom.

$$\mathbf{T} = \begin{bmatrix} 1 & 0 & -t_1 \\ 0 & 1 & -t_2 \\ 0 & 0 & 1 \end{bmatrix},$$

$(t_1(n), t_2(n), 1)$ is the pole of vanishing line $\mathbf{l}_\infty$ with respect to conic $\mathbf{C}_n$ on the metric plane. Since the pole is constrained by the rotation axis $\mathbf{l}_s$, only one degree of freedom exists in the translation matrix.

$$\mathbf{S} = \begin{bmatrix} s & 0 & 0 \\ 0 & s & 0 \\ 0 & 0 & 1 \end{bmatrix},$$

After passing the matrices of $\mathbf{P}_u$, $\mathbf{A}$ and $\mathbf{T}$, the conic is transformed into a circle with center at the original point. The isotropic scaling matrix scales the circle to a circle with radius is one. There is one dof for each conic.

Since the rotation matrix does not affect the circle with center at the original point, no degree of free lies in the matrix $\mathbf{R}$ for the circle.

As a conclusion, for the MLE there are six dof for the fixed entities (2 for each circular point, and 2 for $\mathbf{l}_s$) and then 2 for each conic (which correspond to where the centre is on the rotation axis (1) and its radius (1)). The MLE would minimize e.g. the Sampson error (the linear approximation to the geometric error) over $6+2n$ (n is the number of conics) parameters for all points associated with each conic.

The cost function is

$$\mathcal{C} = \sum_n \sum_m d_\perp(\mathbf{x}, \mathbf{C})^2, \tag{4}$$

the first $\sum$ indicates the number of conics and the second indicates the number of points on their corresponding conics.

$$d_\perp(\mathbf{x}, \mathbf{C})^2 = \frac{(\mathbf{x}^T\mathbf{C}\mathbf{x})^2}{4((\mathbf{C}\mathbf{x})_1^2 + (\mathbf{C}\mathbf{x})_2^2)},$$

where $(\mathbf{C}\mathbf{x})_i$ denotes the i-th component of the 3-vector $\mathbf{C}\mathbf{x}$.

The $6+2n$ initial parameters should be selected carefully. Usually several long tracking points are used to initialize the 6 parameters with the method in Section 3. The points track longer than 4 views are selected to fit conics ([**?**], [**?**]). We also can use the method of finding miss points stated in Section 3 to avoid the fitted conic too bad. The poles of each conic with respect to the vanishing line is calculated, the nearest points on the rotation axis are used to calculate the initial values t_1 (1 dof). Now each conic can be translated to a circle. The radius can determine the initial value s (1 dof). Then each conic can be obtained from the circle (radius is one and center on the original point) and the cost function can be minimized using the Levenberg-Marquart numerical algorithm.

5 Experiments

The new algorithm of computing single axis geometry from only conics has been implemented. The whole computational procedure is simple and robust. We just give two examples to demonstrate the method. The first example is from the popular dinosaur sequence from the University of Hannover. In this experiment, we have introduced a robust method for computing the rotation angles. We also show directly the projective meaning of rotation angles in an image plane. Another example is a sequence from a girl in a rotating chair. This example also shows the practicality of this geometrical setting and the easy of computation.

The dinosaur sequence contains 36 views from a turntable with a constant 10 degrees angular motion. The angular accuracy is about 0.05 degrees[**?**]. Figure **??**.a shows the tracking of some interest points and using the MLE, fitting them to conics Figure **??**.b and calculate the rotation angles. Figure **??** shows the results of recovered rotation angles.

Actually, the rotation angles can be labeled on the vanishing line after randomly selecting a reference point. For instance, we may select the cross point of lines $\mathbf{l}_\infty$ and $\mathbf{l}_s$ in Figure **??** as the reference point with the rotation angle is zero. Any rotation angle can then be computed directly by applying Laguerre's

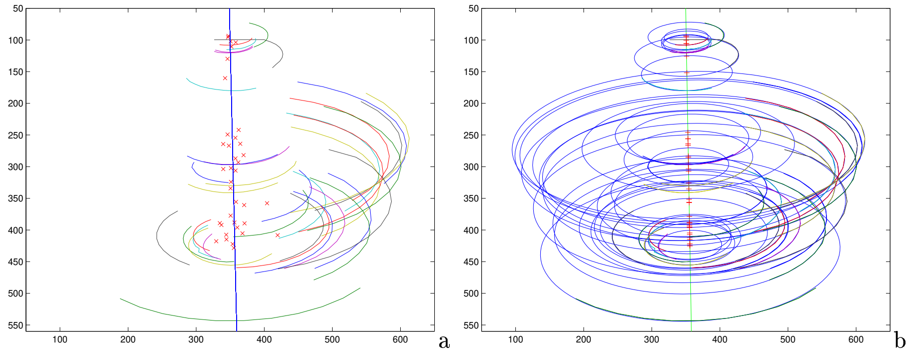

Fig. 6. (a)Tracked points. Some points tracked from the dinosaur sequence. The marks of '×' are initial poles of the direct fitted conics with respected to the vanishing line. (b)Fitted conics with the MLE. The marks of '+' are poles of the MLE fitted conics with respected to the vanishing line. The marks '+' are nearly on the rotation axis.

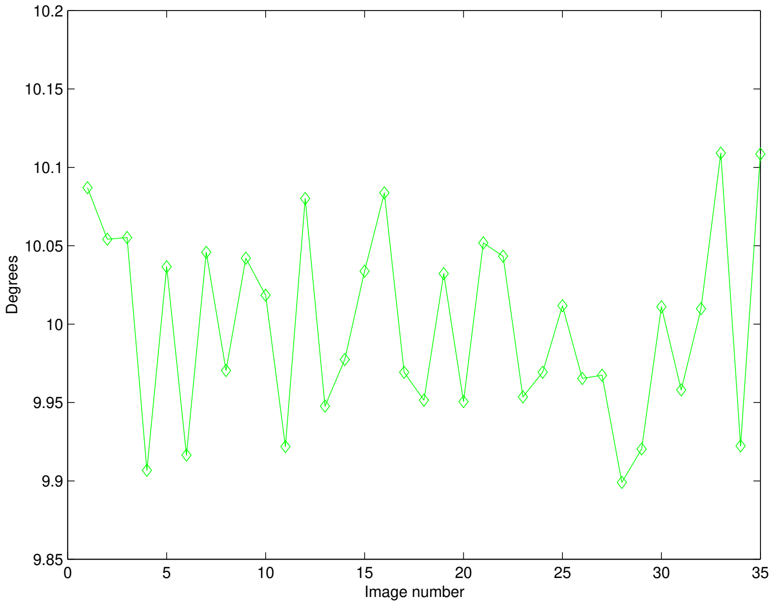

Fig. 7. Recovered rotation angles for the whole sequence of 36 views.

formula and labeled on the vanishing line. After knowing the rotation angles in 36 views, for each point on the dinosaur, if its conic locus has been estimated and one cross point of the line $\mathbf{l}_\infty$ and the line connecting one tracked point on the conic and the pole of the conic with respected to the vanishing line is known, the 36 rotation angles with respected to the reference point can be marked in the vanishing line. Then, the corresponding points in all 36 views (Figure **??**) can be determined.

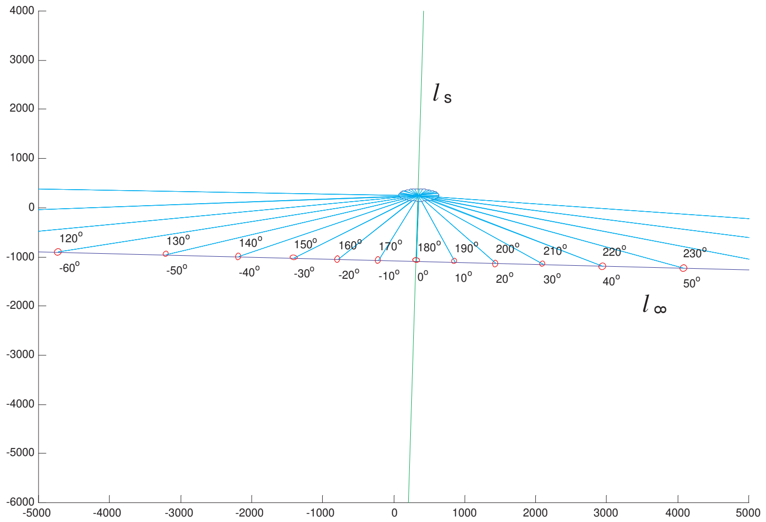

Fig. 8. Labeled rotation angles on the vanishing line (Dinosaur sequence). Select one reference point on the vanishing line, any rotation angle can be labeled on the vanishing line according to the Laguerre's formula.

Using Shape-from-Silhouettes approach mentioned by authors [**?**],[**?**], the horizontal slices of the dinosaur model can be obtained as illustrated in Figure **??**. As the $\mathbf{v}$ is unknown, there remains unknown ratios among slices and the reconstruction is up to two projective parameters as shown in Figure **??**.

With a reasonable choice of the ratio, full reconstruction is obtained as illustrated in Figure **??**.

In the second example of a girl in a rotating chair. The reconstruction is done with a short time video sequence. Figure **??** shows three images captured from the video. A vertical line in the background (Figure **??**.c) is used for locating the vanishing point $\mathbf{v}$ along the rotation axis and we also assume the camera aspect ratio is one. Figure **??** shows the reconstructed 3D points in different views. Figure **??** shows the reconstructed girl.

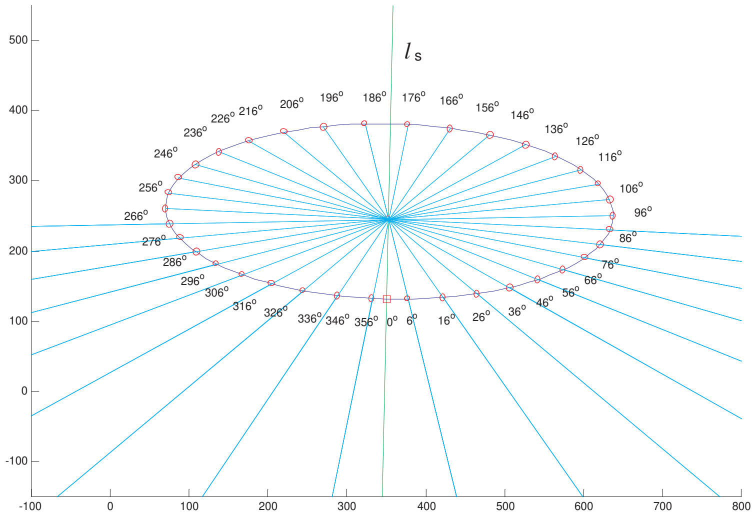

Fig. 9. Recovered corresponding points on one conic (Dinosaur sequence). After knowing the rotation angles in 36 views, with the fitted conic and a point on the conic, the corresponding points in 36 views can be recovered.

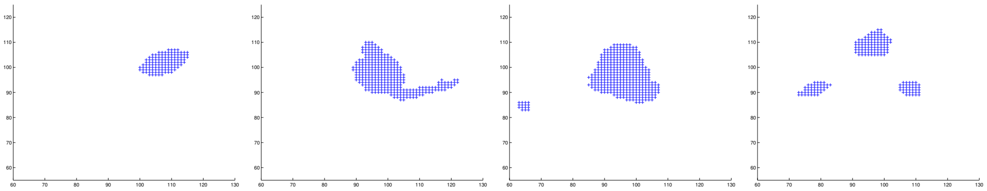

Fig. 10. Four Slices of the dinosaur.

Fig. 11. 3D reconstruction up to two projective parameters. Four reconstructions are displayed with different choices of unknown parameters.

Fig. 12. Reconstructed dinosaur.

Fig. 13. Three images captured from the video. The video is a girl in a rotating chair. A vertical line in the background is marked out for searching the vanishing point along the rotation axis.

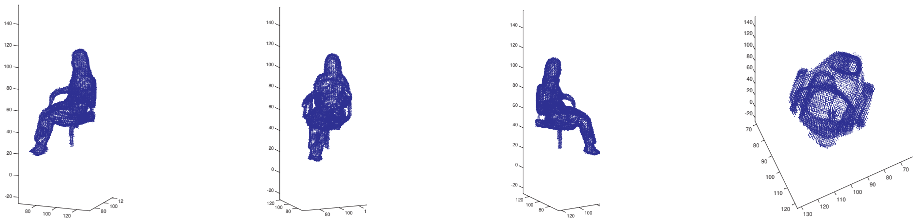

Fig. 14. 3D points of reconstructed girl from four different views.

Fig. 15. Reconstructed girl.

6 Conclusion

We have presented a novel intuitive method of computing single axis geometry by only fitting conic loci to the corresponding points. The novelty of this algorithm is that it does not need to calculate any multiple view geometry such as fundamental matrices and trifocal tensors. Compared with our previous related work in which we need to compute one fundamental matrix and one conic, we need to compute only two, or at least three conics without any other geometric quantities in our new approach. The algorithm is much more simple and robust as the number of parameters to be estimated has been substantially reduced. This fact is verified by some real experiments showing good results for our algorithm.

References

1. L. de Agapito, R. Hartley, and E. Hayman: Linear self-calibration of a rotating and zooming camera, *CVPR*, Vol. 1, pp. 15-21, 1999.
2. M. Armstrong, A. Zisserman, and R. Hartley: Self-Calibration from Image Triplets, *ECCV*, pp. 3-16, 1996.
3. F. Bookstein: Fitting conic sections to scattered data, *CVGIP*, vol. 9, pp. 56-71, 1979.
4. E. Boyer: Object models from contour sequences, *ECCV*, pp. 109-118, 1996.
5. C.H. Chien and J.K. Aggarwal: Identification of 3D objects from multiple silhouettes using quadtrees/octrees. *Comp. Vision, Graphics, and Image Processing* 36, 1986, pp.256-273.
6. R. Cipolla, K.E. Astrom, and P.J. Giblin: Motion from the frontier of curved surfaces, *In Proc. 5th Int. Conf. on Computer Vision*, pp. 269-275, 1995.
7. O. Faugeras: Stratification of three-dimensional vision: projective, affine, and metric representation. *J. Opt. Soc. Am., A*, Vol. 12, pp. 465-484, 1995.

8. A. Fitzgibbon, M. Pilu, and R.B. Fisher: Direct least square fitting of ellipses. *PAMI*, Vol. 21, No. 5, pp. 476-480, 1999.
9. A.W. Fitzgibbon, G. Cross, and A. Zisserman: Automatic 3D Model Construction for Turn-Table Sequences, *SMILE Workshop*, Freiburg, Germany, pp. 155-170, 1998.
10. A.W. Fitzgibbon, and A. Zisserman: Automatic Camera Recovery for Closed or Open Image Sequences, *ECCV*, pp. 311-326, 1998.
11. A.W. Fitzgibbon, and A. Zisserman: Automatic 3D Model Acquisition and Generation of New Images from Video Sequences, *EUSIPCO '98*, Rhodes, Greece, pp. 1261-1269, 1998.
12. R. Hartley: Euclidean reconstruction from uncalibrated views, *In J. Mundy, A. Zisserman, and D. Forsyth, editors, Applications of Invariance in Computer Vision*, LNCS 825, SpringerVerlag, pp. 237-256, 1994.
13. R. Hartley and A. Zisserman: Multiple View Geometry in Computer Vision, *Cambridge Uinversity Press*, 2000.
14. J.J. Koenderink and A.J. van Doorn: Affine structure from motion. *J. Opt. Soc. Am., A*, 8(2), pp. 377-385, 1991.
15. D. Liebowitz and A. Zisserman: Metric rectification for perspective images of planes. *CVPR*, pp. 482-488, 1998.
16. Q.-T. Luong and O.D. Faugeras: The Fundamental matrix: theory, algorithms, and stability analysis, *IJCV*, pp. 43-76, 1996.
17. P.R.S. Mendonça, K.-Y.K. Wong, and R. Cipolla: Camera pose estimation and reconstruction from image profiles under circular motion. *In D. Vernon, editor, Proc. 6th European Conf. on Computer Vision*, volume II, pp. 864-877, Dublin, Ireland, Jun 2000. Springer-Verlag.
18. J. Mundy, and A. Zisserman: Repeated Structures: Image Correspondence Constraints and Ambiguity of 3D Reconstruction, *In Applications of invariance in computer vision*, SpringerVerlag, 1994.
19. W.Niem: Robust and Fast Modelling of 3D Natural Objects from Multiple Views, *SPIE*, San Jose, Vol. 2182, pp. 388-397, 1994.
20. W. Niem, and R. Buschmann: Automatic Modelling of 3D Natural Objects from Multiple Views, *Yakup Paker and Sylvia Wilbur: Image Processing for Broadcast and Video Production. Workshops in computing series*, Springer, Hamburg, 1994.
21. H.S. Sawhney, J. Oliensis, and A.R. Hanson: Image Description and 3-D Reconstruction from Image Trajectories of Rotational Motion. *PAMI*, Vol. 15, No. 9, pp. 885-898, 1993.
22. J. Semple, and G. Kneebone: Algebraic Projective Geometry. *Oxford University Press*, 1952.
23. P.F. Sturm, and S.J. Maybank: On plane-based camera calibration: A general algorithm, singularities, applications, *CVPR*, pp. 432-437, 1999.
24. S. Sullivan, and J. Ponce: Automatic model construction, pose estimation, and object recognition from photographs using triangular splines, *PAMI*, Vol. 20, No. 10, pp. 1091-1097, 1998.
25. R. Szeliski: Shape from rotation, *CVPR*, pp. 625-630, 1991.
26. A. Zisserman, D. Liebowitz, and M. Armstrong: Resolving Ambiguities in Auto-Calibration, *In Philosophical Transactions of the Royal Society of London*, SERIES A, vol. 356, no. 1740, pp. 1193-1211, 1998.
27. Related work.